UNIVERSITI
MALAYSIA
PERLIS

# Comparison Measurements of Low Resistance and High Strength on Synthesis Graphene Conductive Ink Filled Epoxy

Ameeruz Kamal Ab Wahid[1], Mohd Azli Salim[2,3,4*], Nor Azmmi Masripan[2,3,4], Chonlatee Photong[5] and Adzni Md. Saad[2,4]

[1]Jabatan Kejuruteraan Mekanikal, Politeknik Sultan Azlan Shah, Behrang Stesyen, 35950 Behrang, Perak, Malaysia.
[2]Fakulti Kejuruteraan Mekanikal, Universiti Teknikal Malaysia Melaka, Hang Tuah Jaya Durian Tunggal, 76100 Melaka, Malaysia
[3]Advanced Manufacturing Centre, Universiti Teknikal Malaysia Melaka, Hang Tuah Jaya, 76100 Durian Tunggal, Melaka, Malaysia.
[4]Intelligent Engineering Technology Services Sdn. Bhd., No.1, Jalan TU43, Taman Tasik Utama, 76450 Ayer Keroh, Melaka, Malaysia
[5] Graduate School, Mahasarakham University, Khamriang Sub-District, Kantarawichai District, Maha Sarakham 44150, Thailand

## ABSTRACT

*Stretchable and conductive materials are expected to be widely used for various electronic equipment in the future especially in the field of automotive safety. Flexibility and expandability are the main features of the Stretchable Conductive Ink (SCI) while maintaining the high conductivity levels and can be applied to electronic circuits in vehicles especially for driver health monitoring systems. The experimental work obtained the suitable formulation of the conductive ink based on the resistivity and elasticity values. Five different percentages of samples, 10 wt.% until 30 wt.% with each sample interval represents 5 wt.%. Samples of 20 wt.%, 25 wt.%, and 30 wt.% did not show significant differences in terms of the average volume of resistivity. Filler loading of 25 wt. % of GNP in the filler loading matrix produced the best results for nanomechanical properties. Low resistance and high elasticity of SCI in the vehicle electronic equipment can monitor more effectively the driver's health as SCI can be stretched according to the shape of the human body. It also has good conductivity to measure the movement of the human pulse and muscles.*

**KEYWORDS**: Conductive inks, graphene formulation, resistivity, elasticity, epoxy/graphene mixtures

## 1. INTRODUCTION

Stretchable and conductive materials have been widely used in electronic equipment and health care. It is also expected to be widely used for various electronic equipment in the future especially in automotive safety. Flexibility and expandability are the main features of the Stretchable Conductive Ink (SCI) while maintaining low resistivity levels. The low resistance changes, the better for stretchability [1]. Numerous types of conductive inks with unique fillers have been developed for the development of conductive patterns, such as polymers, carbon nanotubes, and metal nanoparticles or organic metal complexes [2]. The layout of a standard driver health monitoring system is designed to continuously monitor parameters related to drivers, vehicles, and the environment by obtaining data from a variety of sensors and taken from the driver's body, interior, and exterior of the vehicle. Different types of drivers give different results due to the detection of mechanical pressure and strain, temperature variations, and bio-potential changes in the human body.

Graphene has the greatest potential as a high-performance absorption material due to its many attractive properties, including unique structure effects, high specific surface area, and high conductivity [3]. The available screen-printed CI when this research started exhibits very limited stretchability and cannot be used in applications that require flexibility and stretchability. One major challenge of graphene CI is to formulate a suitable ink formulation that can be printed using doctor-blading-based methods. The development of graphene-based inks is mainly focusing on the relevant material, ink preparation, and optimization of conductivity. Because of the strong van der Waals forces between adjacent layers, the graphene sheets are inherently stacked together. Then, it is difficult to exfoliate and distribute graphite nanosheets evenly into a polymer matrix [4].

An experimental investigation was conducted to explore suitable graphene formulation, filler loading, and elasticity. The composition of graphene inks such as filler, solvent, and additives requires proper fluidic properties with specific viscosity and surface tension. It allows the available instrumentation to be used in printing the inks that have low volatilizing temperature and strong adhesion to layers. These features permit the widespread usage of the inks on different substrates, portraying their superior versatility and stretchability characteristics [5].

## 1.1    Previous Studies

Graphene is considered to be a very promising ink material for flexible electronics, with high charge carrier mobility, superlative thermal and chemical stability and intrinsic flexibility [6]. Recent research has concentrated on composite materials based on graphene/metal to enhance the conductivity of pure graphene ink. [7] prepared graphene conductive ink to peel off the adjacent layers of bulk graphite and induce exfoliation using ultra-sonication or under high shear rate, high energy fluctuations or high shear powers. Using Dimethylformamide (DMF), they stabilize the graphene to decrease intermolecular attraction, thereby showing a sheet resistance of $2 \times 10^5$ R/sq. with a curing condition of 400 °C for a few hours to improve the stability of graphene dispersion.
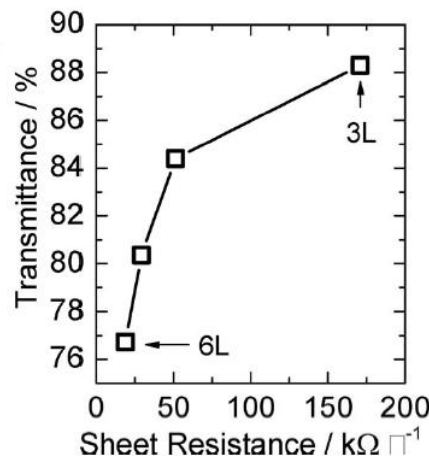


**Figure 1.** Graphene sheet resistance [7].

[8] prepared graphene conductive ink from 1 to 12 wt.% filler loading to test Young's modulus and hardness using the nanoindentation technique introduced by [9]. They measured the hardness and elastic modulus defined directly from indentation load and displacement curves with indentation maximum force of 100 mN, thereby showing Young's modulus and hardness results of 3.5 to 3.75 GPa and 175 to 200 MPa respectively.
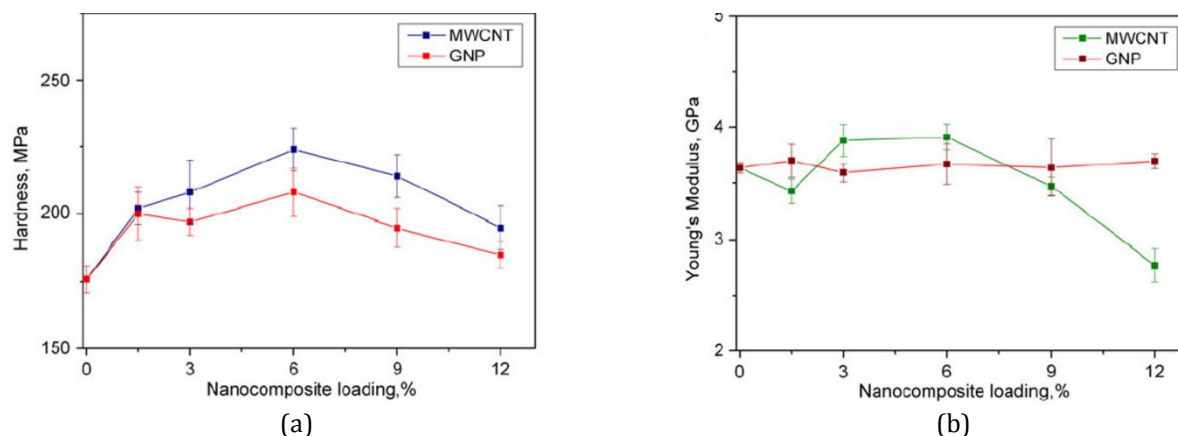
**Figure 2.** Mean values of (a) hardness and
(b) Young's modulus of elasticity versus mono-filler content [8].

## 2.    EXPERIMENTAL METHODS

### 2.1    Synthesis of Graphene Inks

Graphene nanoplatelets powder (GNP) as filler element, Araldite as epoxy resin, and Polytheramine as hardener were used as the main materials for this research, which received without further modification. All raw materials (GNP, epoxy, and hardener) were precisely weighted using the thinky mixer machine.

Graphene as a filler is a potential material to be used in the next generation of electronic devices, composite materials, and energy storage devices due to its outstanding electrical, mechanical, and thermal properties [10]. The use of graphene as a filler element is desirable because of its low cost and high electrical conductivity, which is suitable for industrial-scale production [11]. The properties of GNP available from the product datasheet are presented in Table 1.

**Table 1** Properties of GNP

| Specification | |
|---|---|
| Form | Powder |
| Surface area | 50-80 $m^2/g$ |
| Average flake thickness | 15 nm |
| Average particle size | 5 μm |
| Density | 0.03 – 0.1 $g/cm^3$ |

Araldite was an epoxy resin used for embedding. The epoxy resin is colorless and composed of Araldite, dodecenyl succinic anhydride, dibutyl phthalate, and 2, 4, 6-tridimethylamine methyl phenol. Polytheramine, as a hardener was used to harden or dry the mixtures of the formulations. The hardener is a necessary liquid substance to maintain the viscosity of CI for all forms of printing. Polytheramine is an amine group type of curing agent that provides tough, clear, coatings, castings, and adhesives.

### 2.2    Preparation of Graphene Conductive Ink Formulation

The formulation materials for the experiments were prepared and added accordingly to the predefined ratio inside a container starting with GNP powder. The formulations contained 0.5 g of resin and hardener. Table 3 tabulates five samples starting with 10-30 wt.% with each

sample interval of 5 wt.% and followed by mixing with 70-90 wt.% of binder (epoxy) and hardener (30% of epoxy weight). The conductive ink typically includes between 40-60% of conductive particles and between 30-50% of binder. The stretchable conductive ink patterns can be stretched more than twice their length without breaking or rupturing [12].

The added materials were accurately weighed using the thinky mixer machine and followed by a mixing process with a rotational speed of 2000 rpm for three minutes. The thinky mixer was also used for the removal of invisible micron-sized bubbles. Shear mixing assistance in the liquid media directly exfoliates the raw graphite materials into graphene. Its advantages include the low cost, the processability of the solution, and the resulting footprints have excellent conductivity [5].

This study used a microscope glass slide as a substrate for the CI with a size of 2.54 cm x 7.62 cm and 0.1 cm - 0.12 cm of thickness. The use of glass substrates in the experiment was for the measurement of electrical conductivity because of their thermal stability over the entire temperature range and high insulation property [13].

**Table 2** Formulation of the Materials in The Development of the Conductive Ink

| Sample | GNP | | Epoxy | | Hardener (g) |
|---|---|---|---|---|---|
| | (wt.%) | (g) | (wt.%) | (g) | |
| S10 | 10 | 0.050 | 90 | 0.450 | 0.135 |
| S15 | 15 | 0.075 | 85 | 0.425 | 0.128 |
| S20 | 20 | 0.100 | 80 | 0.400 | 0.120 |
| S25 | 25 | 0.125 | 75 | 0.375 | 0.113 |
| S30 | 30 | 0.150 | 70 | 0.350 | 0.105 |

As shown in Figure 3 below, the patterns of thick layer dimensions of 3.0 mm (width, w) x 25.4 mm (length, l) x 0.1 mm (thickness, $t_s$) were printed on the glass slide. The samples were prepared precisely according to every applicable test to evaluate certain characterizations.
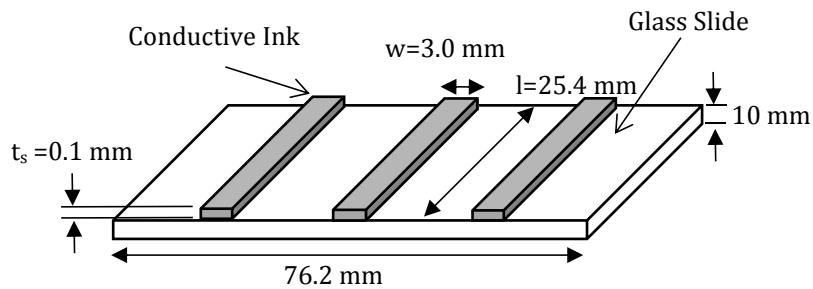


**Figure 3.** Pattern of thick layer dimension of conductive ink on the glass slide.

The commonly used method for the curing process is heating in an oven. The sample was placed in an oven and set at an appropriate temperature and time to avoid damaging the formulated material and substrates. This method used at low temperatures also helped in reducing the time of the curing and also diversifying the types of substrates that can be used [14]. Several studies had been carried out to find the low sheet resistance, which is time-consuming and not economically viable for mass production [11].

After the curing process, the following process was normalizing all specimens at room temperature for about 24 hours and then, the specimen was placed inside the desiccator.

Normalizing is the process of heating a material to a temperature above a critical limit and then cooling it in the open air. The objective of normalizing the heat temperature is to improve the material's mechanical properties by optimizing the microstructure.

## 2.3 Electrical Characterization Method

This experiment focuses on finding the ability of electrical conductivity through CI to be used in circuits. The electrical conductivity of a circuit is determined by the resistance of the material used to produce the circuit. Materials that are used to produce a circuit is depending on the mixture of materials that have different percentages. The percentage differences in the formulations produce different sheet resistance values. They were measured by using a four-terminal (4T) sensing method under room temperature using In-Line Four-Point Probe, with an input range between 10 nA to 100 mA at three different locations per stripes, which equal to 9 data per sample. Then, the data were calculated to get a volume of resistivity for all samples of thick layers, which were then converted into one average value.

## 2.4 Mechanical Characterization Method

The significance of the mechanical properties, which as important as the electrical properties is to determine the strength performance reliability of the material. The hardness of CI samples was tested using a nano-indentation machine. Nano-indentation depth must be adjusted carefully to avoid crack and rupture of the formulation and consequently loss of protective effect [15]. In determining the suitable elasticity modulus, 150 mN nano-indentation force value was tested for all samples. The resulting elasticity of this experiment was the average values taken at three different points on the sample surface.

In this experiment, a typical indentation experiment consists of the following steps: (1) approaching the surface, (2) loading to the peak load of 150 mN, (3) holding the indenter at peak load for 5 s, (4) unloading from the maximum force of 150 mN, and (5) completing the unloading process. The holding step was included to avoid the influence of the creep on the unloading characteristics since the unloading curve was used to obtain the elastic modulus of the material. One particularly important observation resulting from this experiment is concerning the shape of the hardness impression after the indenter is unloaded and the material elastically recovers. In nanocomposite materials, the equal loadings have made a strong and stable contribution to the nanomechanical properties [8].

## 3. RESULTS AND DISCUSSION

## 3.1 Electrical Characterization Analysis

The measurements of resistivity (average sheet resistance, the average volume of resistivity and standard deviation values) of different percentages of filler loading percentage are presented in Table 3. S10 and S15 samples representing GNP of 10 wt.% and 15 wt.%, respectively showed very high values of sheet resistance, the volume of resistivity, and standard deviation. The loss modulus is higher for both 10 wt.% and 15 wt.% of graphene than the storage modulus throughout the range of stresses measured, indicating that these formulations display liquid-like behavior [16]. Results for samples S20 ($4.1799 \times 10^3$ R/sq), S25 ($3.9784 \times 10^3$ R/sq), and S30 ($2.1655 \times 10^3$ R/sq) do not show a significant difference between the results because the binder content used is less for these samples, it makes the samples to possess less liquidity behavior after the curing process. The results are better than what is available in the literature [7] for graphene conductive ink that using DMF to stabilize the graphene ink and not screen printed.

**Table 3** Measurement of Resistivity

| Sample | Sheet Resistance, Average, (R/sq) | Volume of Resistivity, Average, (Ω.cm) | Standard Deviation (Ω.cm) |
|--------|-----------------------------------|----------------------------------------|---------------------------|
| S10 | $55.5161 \times 10^6$ | $330.7764 \times 10^3$ | $296.8148 \times 10^3$ |
| S15 | $1.1436 \times 10^6$ | $6.8139 \times 10^3$ | $1.5557 \times 10^3$ |
| S20 | $4.1799 \times 10^3$ | 24.9046 | 4.4328 |
| S25 | $3.9784 \times 10^3$ | 23.7043 | 3.5152 |
| S30 | $2.1655 \times 10^3$ | 12.9024 | 3.2456 |

From the results in Figure 4, the graph illustrates very large difference of the value for standard deviation between sample of 10 wt.% to the other samples. It is because, the filler loading at 10 wt.% has too little graphene content, which causes the resistance on the sample to be unstable and too high as compared to other filler loading percentages. Starting from 20 wt.% until 30 wt.%, each of the samples is having a small standard deviation value because the percentage of graphene can balance the entire pattern on the sample. It causes the resistance of the whole pattern does not have a significant difference. However, the average volume of resistivity between 15 wt.% and 20 wt.% is significantly different, with values of $6.8139 \times 10^3$ Ω.cm and 24.9046 Ω.cm, respectively. This makes the GNP material at 15 wt.% is also rejected because of the high resistance. Samples of 20 wt.%, 25 wt.%, and 30 wt.% do not show significant differences in term of the average volume of resistivity and also do not significantly affect the flow rate in the circuit.
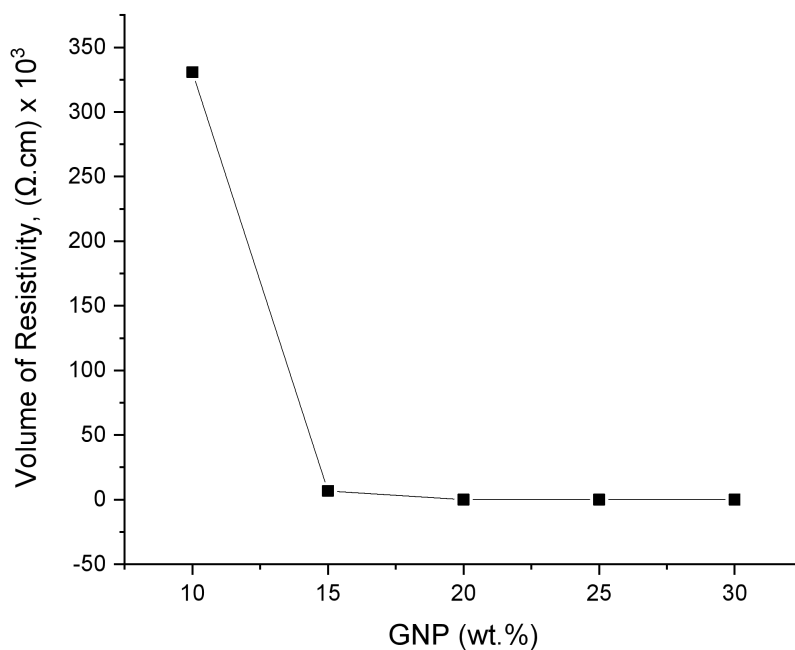


**Figure 4.** Volume of resistivity (Ω.cm) on conductive ink formulation.

## 3.2    Mechanical Characterization Analysis

The hardness and elastic modulus were calculated from the recorded load-displacement curves using [9] method. Mechanical properties were directly determined by the indentation load and displacement measurements without the need to capture the image of hardness impression. The load was measured as a function of penetration depth. 150 mN nano-indentation force was tested on all samples begin with 10 wt.% until 30 wt.% with the increasing of 10 wt.%.
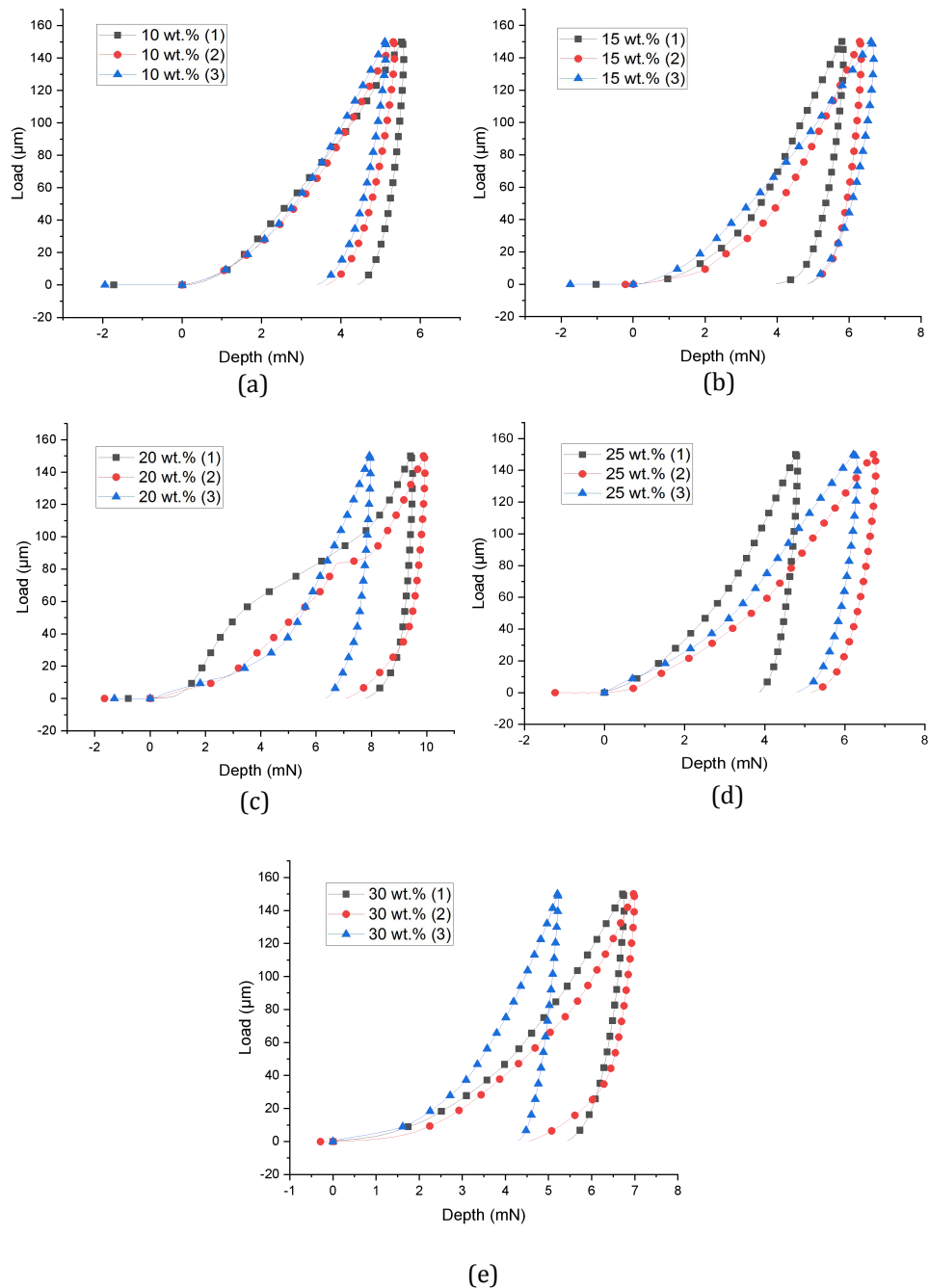
**Figure 5.** Representation of load–displacement curves showing different penetration depths, (a) 10 wt%, (b) 15 wt.%, (c) 20 wt.%, (d) 25 wt.% and (e) 30 wt.%.

Figure 5 shows three different indentation points for each sample of filler loading surface. The three different points are to determine the uniformity of penetration depth at every different filler loading percentages to the hardness and Young's modulus. The nanoindentation test was performed at the maximum force of 150 mN and retention time of 5 s to eliminate the viscoelastic contribution and validate the [9] model. Load-displacement curves in Figure 5 show that 20 wt.% has the highest penetration depth. The resistance to displacement of GNP at fillers loading of 20 wt % has the highest endurance to plastic strain in the reinforced samples as compared to the other filler loading percentages.

**Table 4** Nanoindentation results of different conductive ink filler loadings

| Sample | Average Maximum Depth, $h_{max}$ (μm) | Average Young's Modulus, E (GPa) | Young's Modulus Standard Deviation (GPa) | Average Hardness, HV (MPa) | Hardness Standard Deviation (MPa) |
|---|---|---|---|---|---|
| S10 | 5.226 | 9.52 | 0.593 | 25.01 | 1.258 |
| S15 | 6.250 | 10.5 | 2.17 | 16.41 | 2.228 |
| S20 | 9.095 | 8.59 | 1.41 | 7.59 | 1.92 |
| S25 | 5.922 | 13.8 | 6.509 | 19.06 | 7.137 |
| S30 | 6.311 | 10.7 | 2.495 | 16.95 | 5.996 |

The result shows in Table 4 is taken based on the average of the three different points on the sample surface. The average values of hardness and Young's modulus depending on the nanofiller concentration obtained from nano-indentation tests over a different percentage of CI filler loading are presented in Figures 4(a,b). The result shows that the average Young's modulus and average hardness are within the range 8.59 to 13.8 GPa and 7.59 to 25.01 MPa respectively. The results are better than what is available in the literature [8] for nanoindentation experimental of graphene conductive ink that using 1 to 12 wt.% filler loading with indentation maximum force of 100 mN.
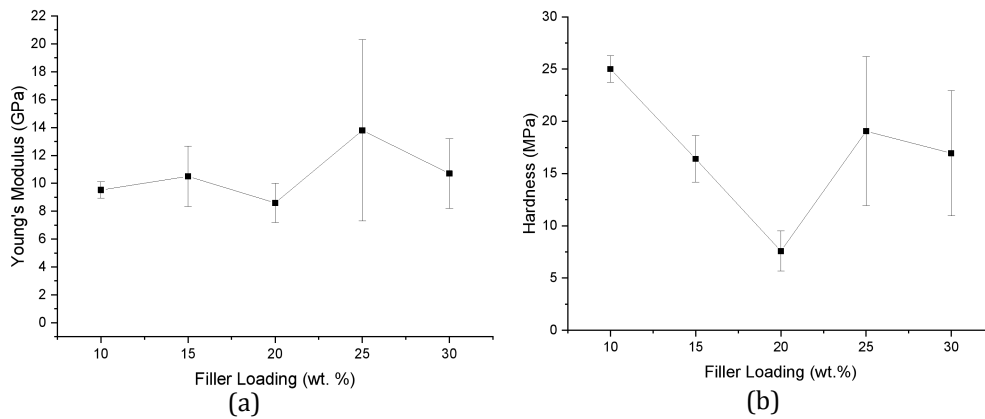


**Figure 6.** Mean values of (a) Young's modulus of elasticity and (b) hardness versus filler loading percentages.

The results show in Figures 6 for hardness and elasticity have the highest standard deviations for 25 wt.% as compared to the other filler loadings. The level of dispersion of the experimental results is significant for the sensibility of the indenter to the inhomogeneity of the composite structure with different percentages of GNP. The experimental errors are within the range ±0.5 to ±6.5 GPa for Young's modulus and ±1.2 to ±7.1 MPa for hardness. It can be observed that 25 wt. % addition of GNP in the filler loading matrix is giving the best results for nanomechanical properties. It is because the filler loading is uniformly dispersed in the CI matrix and no obvious aggregation is observed. The low values for 20 wt.% mono-filled nanocomposites can be explained with the formation of aggregates in the CI structure, resulting in the worst carbon nanofiller dispersion and therefore having low hardness and elasticity. The resistance to displacement of fillers loading 20 wt.% comparing to filler loading 25 wt.% suggests the higher endurance to plastic strain in the reinforced samples.

## 4.   CONCLUSION

The study was carried out successfully in demonstrating the comparative change in resistivity and elasticity caused by different filler loading percentages. It is reasonable to conclude that the graphene conductive ink material only without the involvement of other materials as solvent or stabilizer also has high potential as a stretchable conductor material. This can be explained by a comparison between previous studies that use solvent or stabilizer to decrease intermolecular attraction with a high temperature of the curing process to improve the stability of graphene dispersion. The sample of 25 wt. % of GNP has excellent electrical and mechanical properties which gave low resistance and the highest results in Young's modulus and hardness. Showing that the filler loading was uniformly dispersed in the CI matrix and no obvious aggregation was observed. Low resistance and high elasticity of SCI in-vehicle electronic equipment would benefit the driver, which can monitor more effectively the driver's health. It is because SCI can be stretched according to the shape of the human body and has good conductivity to measure the movement of the human pulse and muscles.

## ACKNOWLEDGEMENT

## REFERENCES

[1]     Zhang, B., Lei, J., Qi, D., Liu, Z., Wang, Y., Xiao, G., & Chen, X. Stretchable conductive fibers based on a cracking control strategy for wearable electronics. *Advanced Functional Materials*, *28*(29), (2018) 1801683.

[2]     Yang, W. & Wang, C. Graphene and the related conductive inks for flexible electronics. *J Mater Chem C,* **4**, (2016) 7193-7207.

[3]     Saad, H., Salim, M. A., Masripan, N. A., Saad, A. M., & Dai, F. Nanoscale graphene nanoparticles conductive ink mechanical performance based on nanoindentation analysis. *International Journal of Nanoelectronics & Materials*, **13**, (2020).

[4]     Xue, G., Zhang, B., Sun, M., Zhang, X., Li, J., Wang, L., & Song, C. Morphology, thermal and mechanical properties of epoxy adhesives containing well-dispersed graphene oxide. *International Journal of Adhesion and Adhesives*, **88**, (2019) pp.11-18.

[5]     Tran, T. S., Dutta, N. K., & Choudhury, N. R. Graphene inks for printed flexible electronics: Graphene dispersions, ink formulations, printing techniques and applications. *Advances in colloid and interface science*, **261,** (2018) pp.41-61.

[6]     Yang, W., & Wang, C. Graphene and the related conductive inks for flexible electronics. *Journal of Materials Chemistry C*, *4*(30), (2016) pp.7193-7207.

[7]     Li, J., Ye, F., Vaziri, S., Muhammed, M., Lemme, M. C., & Östling, M. Efficient inkjet printing of graphene. *Advanced materials*, *25*(29), (2013) pp.3985-3992.

[8]     Batakliev, T., Georgiev, V., Ivanov, E., Kotsilkova, R., Di Maio, R., Silvestre, C., & Cimmino, S. Nanoindentation analysis of 3D printed poly (lactic acid) -based composites reinforced with graphene and multiwall carbon nanotubes. *Journal of Applied Polymer Science*, *136*(13), (2019) 47260.

[9]     Oliver, W. C., & Pharr, G. M. An improved technique for determining hardness and elastic modulus using load and displacement sensing indentation experiments. *Journal of materials research*, *7*(6), (1992) pp.1564-1583.

[10]    Tran, T. S., Park, S. J., Yoo, S. S., Lee, T. R., & Kim, T. High shear-induced exfoliation of graphite into high quality graphene by Taylor–Couette flow. *RSC advances*, *6*(15), (2016) pp.12003-12008.

[11] Pan, K., Fan, Y., Leng, T., Li, J., Xin, Z., Zhang, J., & Hu, Z. Sustainable production of highly conductive multilayer graphene ink for wireless connectivity and IoT applications. *Nature communications*, *9*(1), (2018) pp.1-10.

[12] Longinotti-buitoni, G., & Aliverti, A. *U.S. Patent No. 9,817,440*. Washington, DC: U.S. Patent and Trademark Office, (2017).

[13] Bourlier, Y., Noël, S., Viel, P., Brézard-Oudot, A., Chrétien, P., Franchini, A., & Karam, A. F. Characterization of Nanocomposite Graphene/polymer Films for Electrical Contact Applications. In *2018 IEEE Holm Conference on Electrical Contacts*, (2018) pp.448-455.

[14] Arapov, K., Rubingh, E., Abbel, R., Laven, J., de with, G., & Friedrich, H. Conductive screen printing inks by gelation of graphene dispersions. *Advanced Functional Materials*, *26*(4), (2016) pp.586-593.

[15] Wang, W., Peng, Q., Dai, Y., Qian, Z., & Liu, S. Distinctive nanofriction of graphene coated copper foil. *Computational Materials Science*, *117*, (2016) pp.406-411.

[16] Compton, B. G., Hmeidat, N. S., Pack, R. C., Heres, M. F., & Sangoro, J. R. Electrical and mechanical properties of 3D-printed graphene-reinforced epoxy. *Jom*, *70*(3), (2018) pp.292-297.